Mesoscale Dzyaloshinskii-Moriya Interaction: 1D and 2D Cases

Oleksii M. Volkov[1,2], Tobias Kosub[1], Volodymyr P. Kravchuk[2,3], Denis D. Sheka[4], Jeroen van den Brink[4,5], Yuri Gaididei[2], Ulrich K. Rößler[4], Hagen Fuchs[1], Hans Fangohr[6,7], Jürgen Faßbender[1], Denys Makarov[1]

[1]Helmholtz-Zentrum Dresden-Rossendorf e.V., Institute of Ion Beam Physics and Materials Research, 01328 Dresden, Germany.
[2]Bogolyubov Institute for Theoretical Physics of National Academy of Sciences of Ukraine, 03680 Kyiv, Ukraine
[3]Leibniz-Institute für Festkörper- und Werksrofforschung Dresden (IFW Dresden), D-01171 Dresden, Germany
[4]Taras Shevchenko National University of Kyiv, 01601, Kyiv, Ukraine
[5]Institute for Theoretical Physics, Technical Universitat Dresden, 01069 Dresden, Germany
[6]University of Southampton, Southampton SO17 1BJ, United Kingdom
[7]European XFEL GmbH, Holzkoppel 4, 22869 Schenefeld, Germany

State of the Art: Magnetism in curvilinear geometries

Topical Review: [Streubel et al., Journal of Physics D: Applied Physics **49**, 363001 (2016)]

One dimensional (1D) curvilinear structures

Microhelices: magnetochiral dichroism

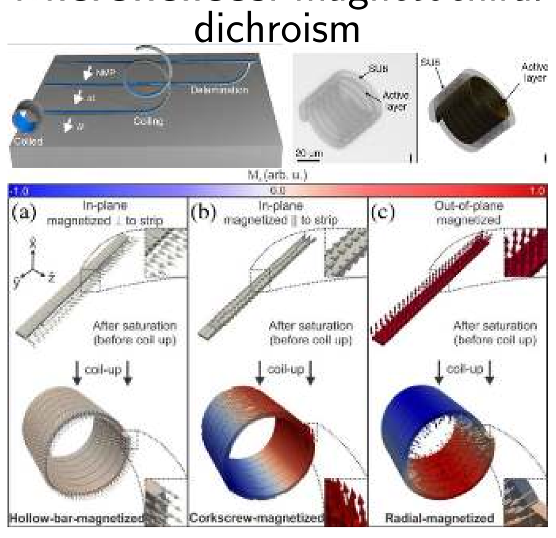

[Smith et al., PRL **107**, 097204 (2011)]

Nanohelices: artificial helimagnets

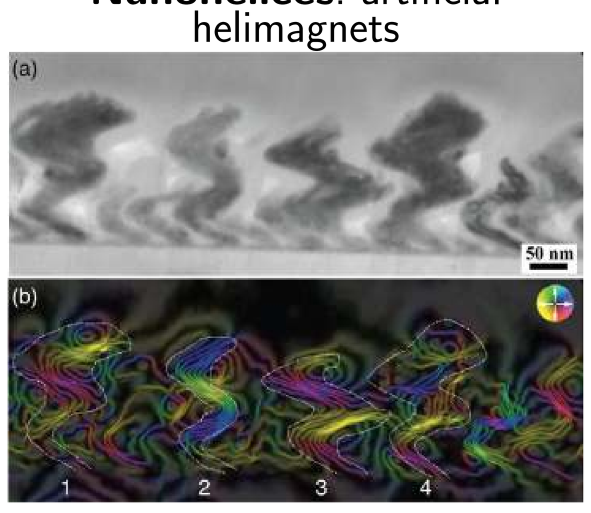

[Phatak et al., Nano Lett. **14**, 759-64 (2014)]

Parabolas: curvature-induced domain wall (DW) pinning

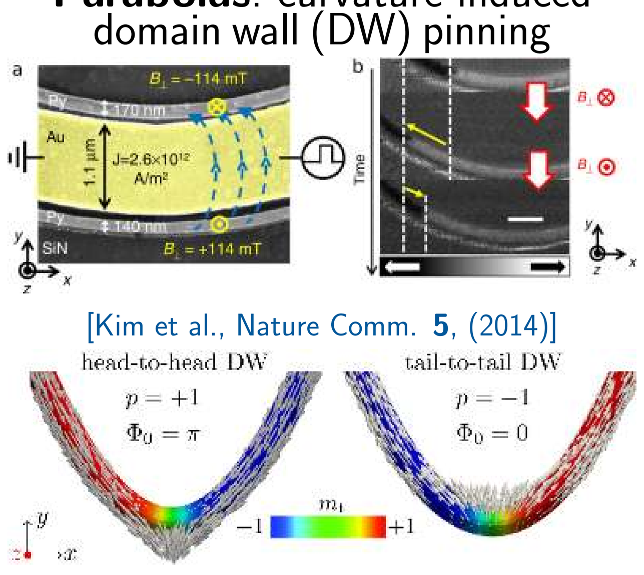

[Kim et al., Nature Comm. **5**, (2014)]

[Yershov et al., Phys. Rev. B **92**, 104412 (2015)]

Two dimensional (2D) curvilinear structures

Nanotubes: ultrafast DW motion

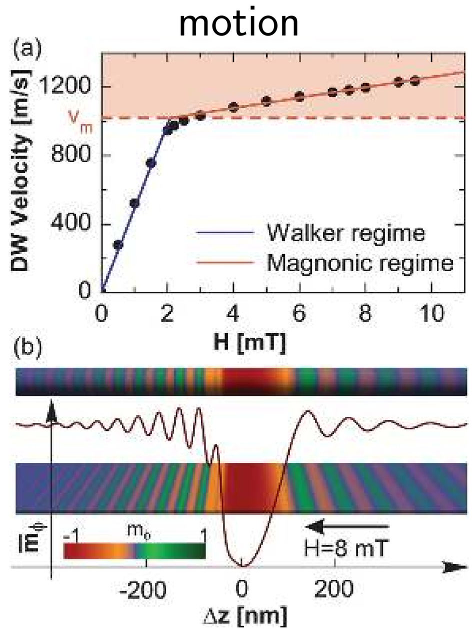

[Yan et al., APL **99**, 122505 (2011)]

Nanocaps: chirality-dependent vortex switching

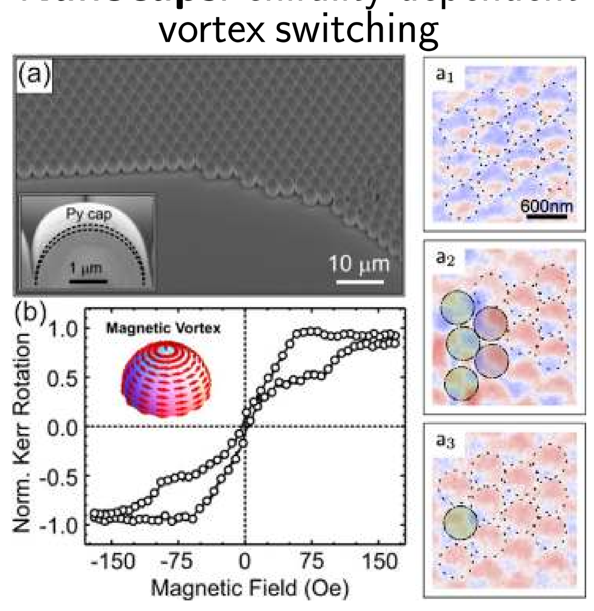

[Streubel et al., PRB **85**, 174429 (2012)]
[Baraban et al., ACS Nano **6**, 3383–9 (2012)]

Möbius stripe: magnetochirality symmetry breaking

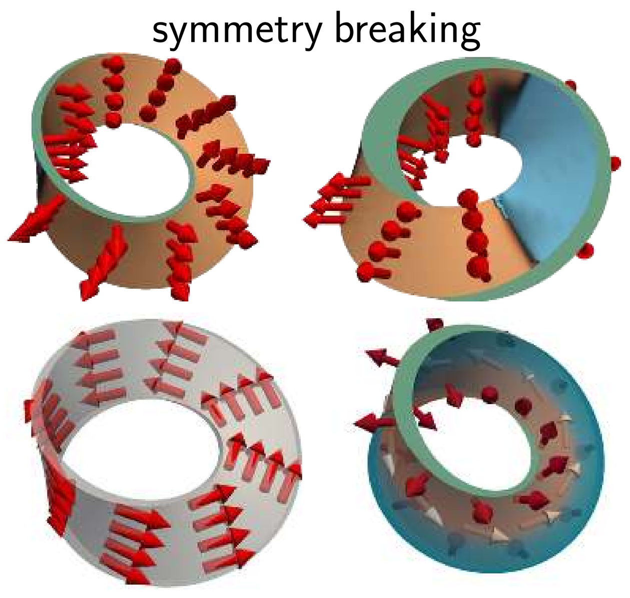

[Pylypovskyi et al., Phys. Rev. Lett. **114**, 197204 (2014)]

Theoretical background for one-dimensional case

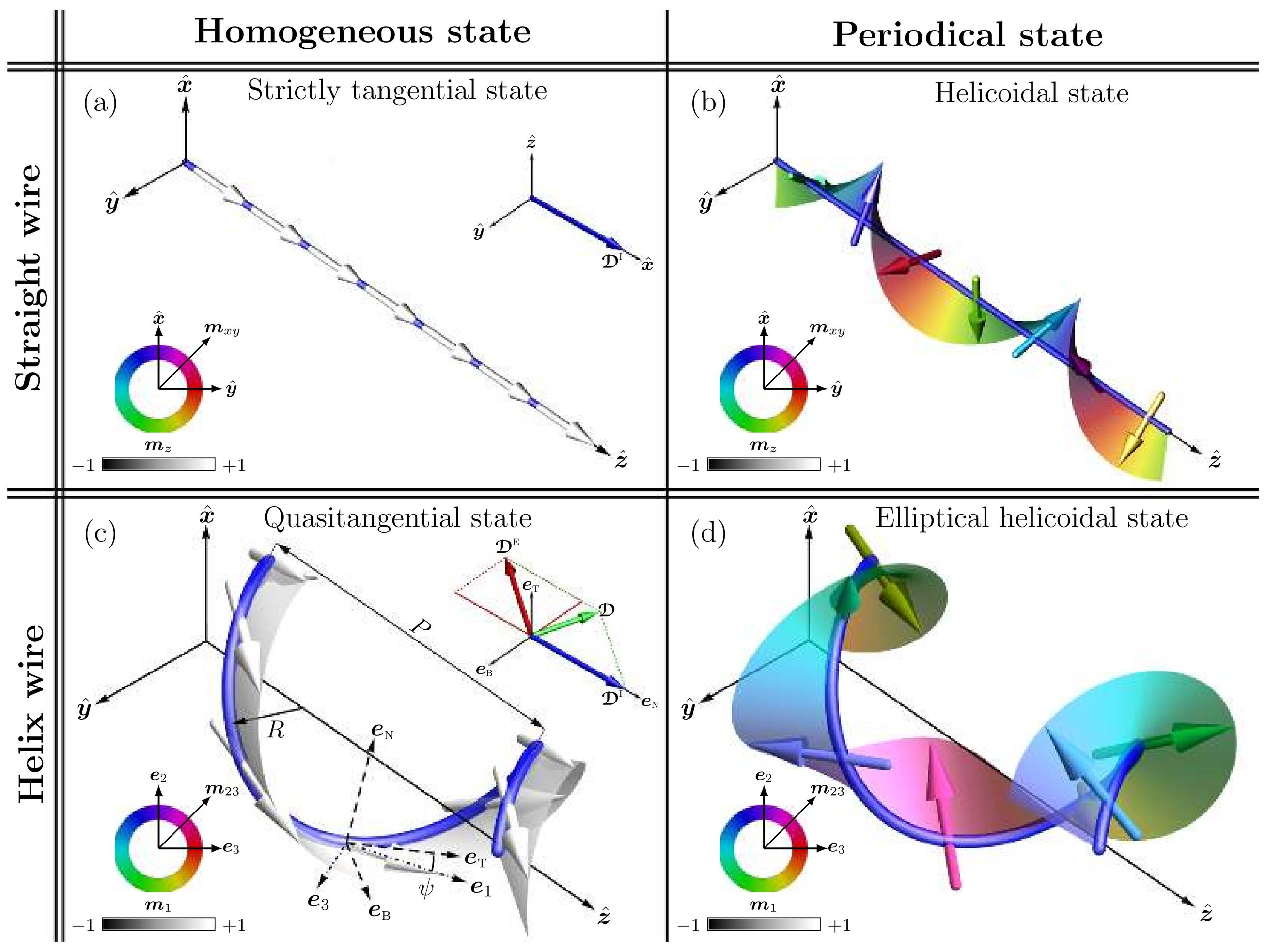

In the case of 1D curvilinear magnetic wire it is convenient to use its natural parametrization by arc length s of a general form $\vec{\gamma} = \vec{\gamma}(s)$ and work in the curvilinear Frenet-Serret (TNB) reference frame $(\vec{e_{\rm T}}, \vec{e_{\rm N}}, \vec{e_{\rm B}})$. The total energy in the TNB reference frame has a form:

$$E = KS \int \mathrm{d}\xi \left\{ m'_\alpha\, m'_\alpha + \mathscr{D}^{\rm meso}_{\alpha\beta} \left(m_\alpha\, m'_\beta - m'_\alpha\, m_\beta\right) + \mathscr{K}^{\rm meso}_{\alpha\beta}\, m_\alpha m_\beta \right\}, \qquad \alpha, \beta = (\mathrm{T}, \mathrm{N}, \mathrm{B}),$$

where $\vec{m}$ is the magnetization unit vector $\vec{m} = \vec{M}/M_s$, with M_s being the saturation magnetization, $()' = \partial_\xi$, with $\xi = s/w$

$$\left\|\mathscr{D}^{\rm meso}_{\alpha\beta}\right\| = \left\| \begin{matrix} 0 & -(\mathcal{D}_{\rm B}/2 - \varkappa(\xi)) & -\mathcal{D}_{\rm N}/2 \\ \mathcal{D}_{\rm B}/2 - \varkappa(\xi) & 0 & -(\mathcal{D}_{\rm T}/2 - \sigma(\xi)) \\ \mathcal{D}_{\rm N}/2 & \mathcal{D}_{\rm T}/2 - \sigma(\xi) & 0 \end{matrix} \right\|,$$

$$\left\|\mathscr{K}^{\rm meso}_{\alpha\beta}\right\| = \left\| \begin{matrix} \sigma(\xi)(\mathcal{D}_{\rm T} - \sigma(\xi)) - 1 & \mathcal{D}_{\rm N}\sigma(\xi)/2 & [\varkappa(\mathcal{D}_{\rm T} - \sigma(\xi)) + \sigma(\xi)(\mathcal{D}_{\rm B} - \varkappa(\xi))]/2 \\ \mathscr{D}_{\rm N}\sigma(\xi)/2 & 0 & \mathcal{D}_{\rm N}\varkappa(\xi)/2 \\ [\varkappa(\xi)(\mathcal{D}_{\rm T} - \sigma(\xi)) + \sigma(\xi)(\mathcal{D}_{\rm B} - \varkappa(\xi))]/2 & \mathcal{D}_{\rm N}\varkappa(\xi)/2 & \varkappa(\xi)(\mathcal{D}_{\rm B} - \varkappa(\xi)) \end{matrix} \right\|,$$

where $K = K_0 + \pi M_s^2$ is the effective anisotropy constant, with $K_0 > 0$, $w = \sqrt{A/K}$ is the characteristic magnetic length, with A being an exchange constant. The tensors $\mathscr{D}^{\rm meso}_{\alpha\beta}$ and $\mathscr{K}^{\rm meso}_{\alpha\beta}$ are mesoscale DMI and anisotropy tensors, respectively, with:

- $\vec{\mathcal{D}}^{\rm I} = (\mathcal{D}^{\rm I}_{\rm T}, \mathcal{D}^{\rm I}_{\rm N}, \mathcal{D}^{\rm I}_{\rm B}) = \vec{D}^{\rm I}/\sqrt{A\,K}$ being the reduced vector of the intrinsic DMI;
- $\vec{\mathcal{D}}^{\rm E} = (-2\,\sigma(\xi),\ 0,\ -2\,\varkappa(\xi))$ is the vector of the extrinsic DMI, with $\sigma = w\,\tau$ and $\varkappa = w\,\kappa$ being the reduced curvature and torsion.

In the following, it is instructive to introduce the vector of the mesoscale DMI:

$$\vec{\mathcal{D}} = \vec{\mathcal{D}}^{\rm I} + \vec{\mathcal{D}}^{\rm E} = (\mathcal{D}^{\rm I}_{\rm T} - 2\sigma,\ \mathcal{D}^{\rm I}_{\rm N},\ \mathcal{D}^{\rm I}_{\rm B} - 2\varkappa).$$

In the case of 2D curvilinear magnetic systems this theory remains valid but becomes more complex, due to differentiation along two orthogonal directions on the curvilinear plane.

Magnetic states on spherical shells

In the case of a thin spherical shell with radius R and easy-normal anisotropy there exist a class of azimuthally symmetric solutions $\vec{m} = \vec{e}_\vartheta \sin\theta + \vec{n}\cos\theta$. The function $\theta = \theta(\vartheta)$ satisfies the following equation:

$$\theta'' + \cot\vartheta\theta' - \sin\theta\cos\theta\left[\frac{\cos 2\vartheta}{\sin^2\vartheta} + \frac{R^2}{w^2} - \frac{4D}{D_c}\right] + 2\cot\vartheta\sin^2\theta\left[1 + \frac{D}{D_c}\right] = 0,$$

where $D_c = 2A/R$ is the strength of the curvature-induced effective DMI that solely is exchange-driven. This geometrical DMI contribution copetes with the intrinsic spin-orbit driven DMI. Full compensation takes place when $D = -D_c$

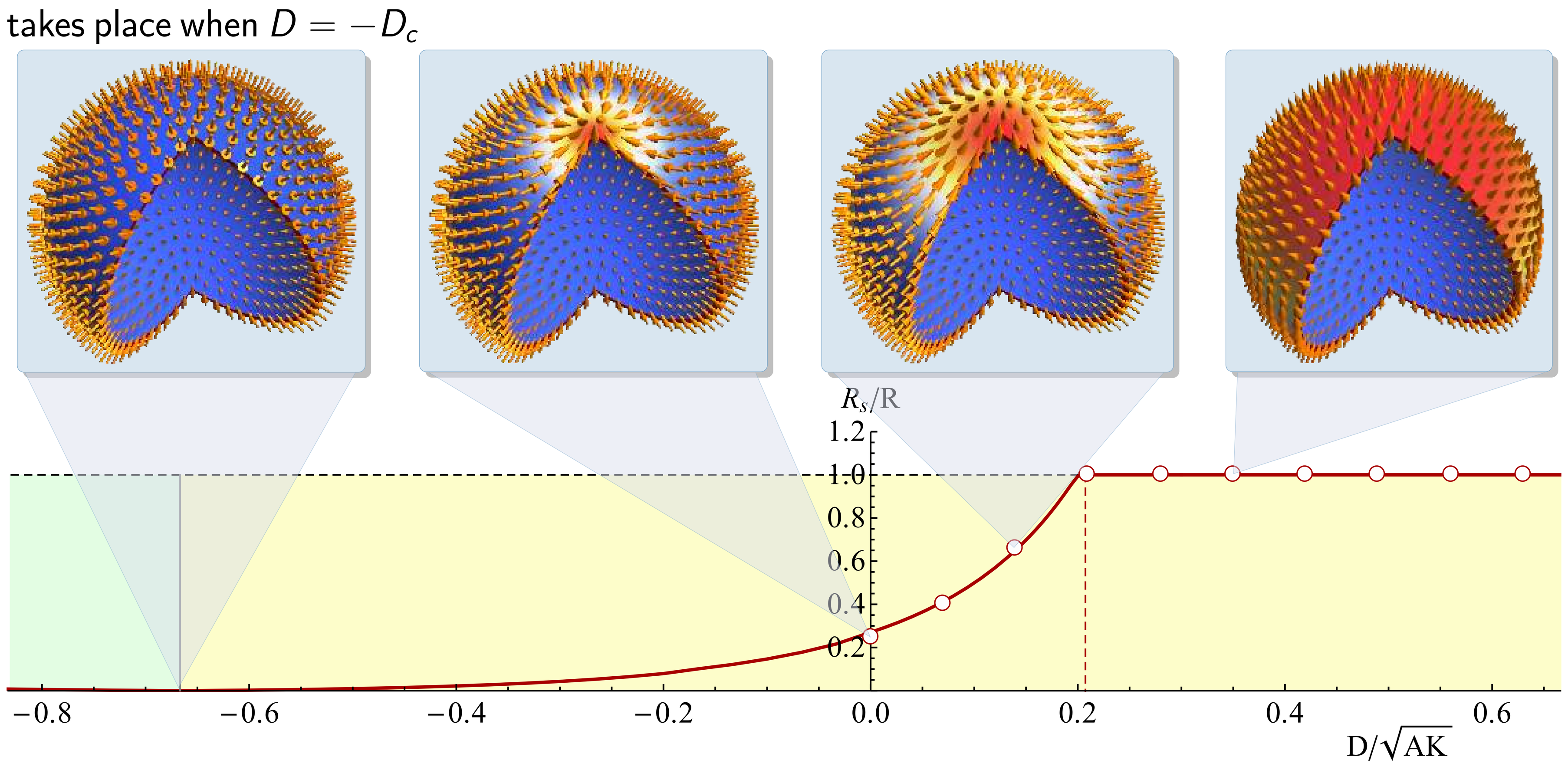

Dependences of the skyrmion radius R_s on the dimensionless DMI constant $\mathcal{D}^{\rm I} = D/\sqrt{AK}$.

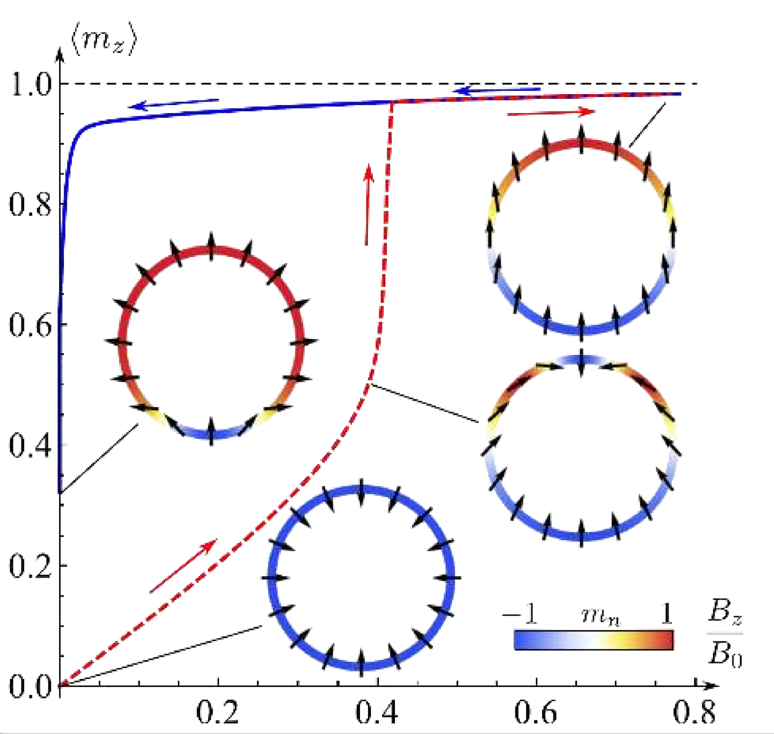

In the case of curvilinear systems resulting skyrmion number $\mathcal{N}$ become dependent on both a magnetic $\mathcal{Q}$ and a geometrical $\mathcal{Q}_g$ topological charges, which provide a topological charge shift:

$$\mathcal{N} = \mathcal{Q} - \mathcal{Q}_g.$$

Thus, for the case of magnetic skyrmion on thin magnetic spherical shell, the corresponding magnetic topological charge $\mathcal{Q} = 0$. Therefore, the skyrmion magnetic configuration can be created by means of a uniform magnetic field.

[Kravchuk, Rößler, Volkov, Sheka, van den Brink, Makarov, Fuchs, Fangohr, Gaididei, Phys. Rev. B **94**, 144402 (2016)]

Microscopic numerical experiments with magnetic wires

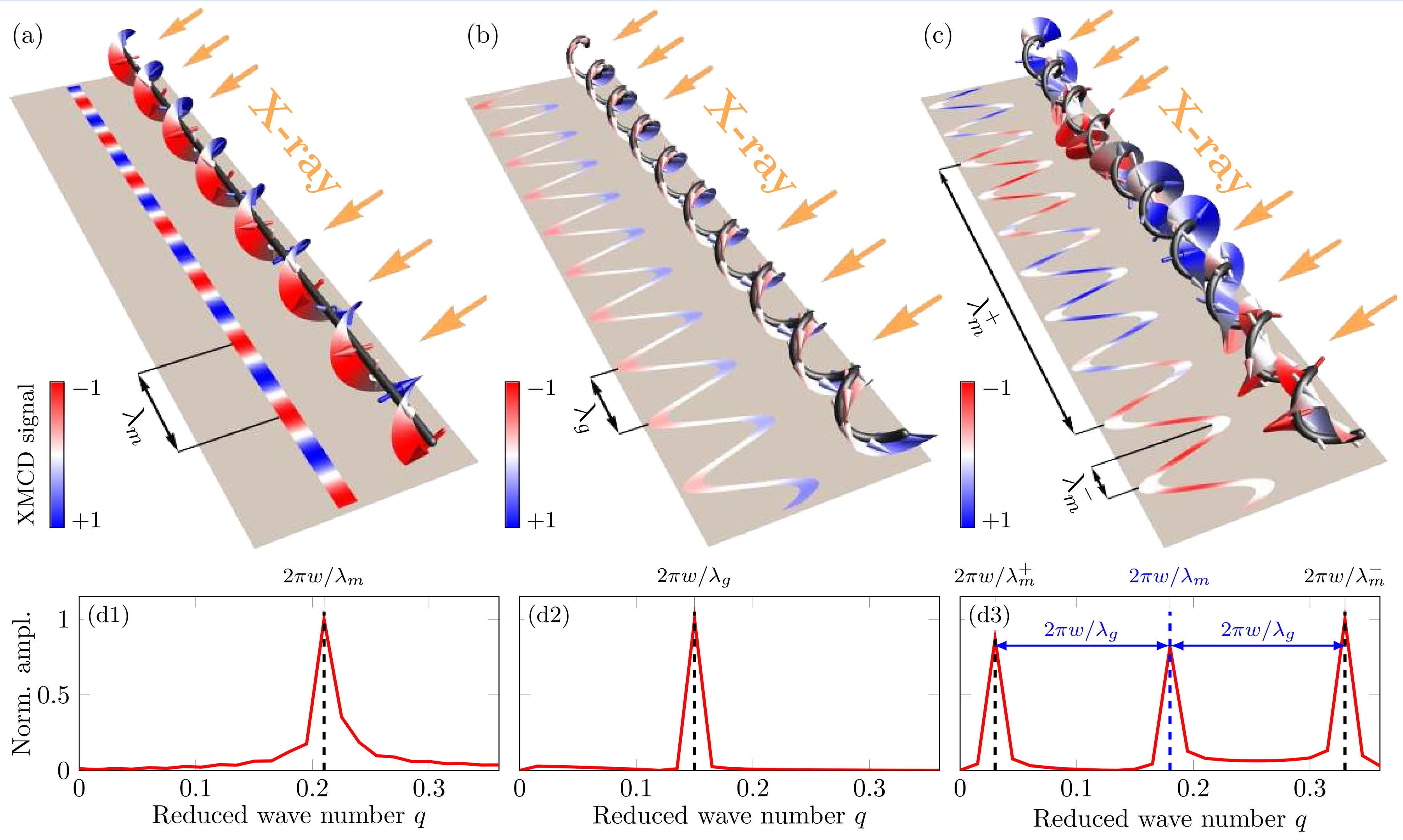

It is possible to access the value for intrinsic DMI from the analysis of the microscopic images of the periodical magnetic states taken by using microscopic techniques, e.g. Lorentz electron microscopy, electron holography, magnetic transmission X-ray microscope (MTXM) and X-ray magnetic circular dichroism photoelectron emission microscope (XMCD-PEEM). We illustrate this possibility for an exemplarily choosen XMCD-PEEM-like experiment, where the x-ray beam hits the samples under the angle of 25° with respect to the surface plane.

(a) The helicoidal state in a straight wire with $\mathcal{D}^{\rm I}_{\rm T} = 2.7$.
(b) The quasitangential state in a helix wire with $\varkappa = 0.8$, $\sigma = 0.5$, $\mathcal{D}^{\rm I}_{\rm T} = 0$, $\mathcal{C} = +1$.
(c) The periodical state with $\varkappa = 0.8$, $\sigma = 0.5$, $\mathcal{D}^{\rm I}_{\rm T} = 2.7$, $\mathcal{C} = +1$.

Colors of the surface of the magnetization rotation and the XMCD-PEEM-like contrast are equal and reveal the magnetization parallel (red) and antiparallel (blue) to the x-ray beam.

(d1-d3) Fourier spectra of the XMCD-PEEM-like signal along the wires for the helicoidal, quasitangential and periodical states, respectively.